

# Strategies for Mitigation of CTE Losses in WFC3/UVIS Images

---

Jay Anderson  
June 8, 2020

---

## ABSTRACT

*Our understanding of the WFC3/UVIS detector continues to improve, even as the detector's charge-transfer efficiency continues to degrade. There is a new pixel-based CTE model that will be introduced into the pipeline shortly. The new model is based on detailed calibration and on-sky observations that show us in detail how variations in background affect the detector's ability to transfer charge efficiently. This will be fully written up in an ISR, but we wanted to bring these considerations to Cy 28 GOs now, so that they can plan their upcoming observations as wisely as possible based on the latest information available.*

---

## 1. Introduction

HST's continued exposure to harsh radiation in its low-earth orbit means that its CCD detectors are subjected to a continued degradation of their CTE (charge-transfer efficiency). This makes mitigation of CTE losses a continually moving target. We have developed a new model for the CTE losses and will soon be releasing it in the pipeline via the pixel-based correction.

The new model differs in a few ways from the previous model. The WFC3/UVIS detector has been in orbit almost twice as long as when the model was previously pinned. "Thanks" to the increased number of warm pixels (WPs) in the detector and the increased CTE-losses of the WPs themselves, with *twice* as much time it becomes *four* times easier to pin down the model. Also, as we understand CTE degradation better, we are in a better position to take optimal calibration data in order to study the aspects of the model that are most relevant to UVIS observations.

This ISR will be a brief discussion of our current understanding of CTE losses. We will be filling out much of this discussion in an upcoming ISR, but we wanted to provide the Cycle 28 GOs the best information possible to plan their observations. It is always the case that preserving charge is preferable to trying to reconstruct or up-correct for what has been lost.

We begin with a discussion of how the CTE model has changed with our increasing knowledge and experience. We then examine how background is able to preserve electrons, both for warm pixels and for actual stars. Armed with this understanding, users are now in a better position to design an observing program to maximize their scientific return.

## 2. The new model

The WFC3/UVIS pixel-based CTE model is based on the treatment in Anderson & Bedin (AB10, 2010), originally developed for ACS. Traps are generated in individual pixels when energetic cosmic rays damage the pixel lattice. These traps are generated at specific locations within specific pixels. The specific location of the trap within its particular pixel will determine how large an electron packet must be in order to be affected by the trap. Traps at the 3-D center of a pixel will affect all charge packages, but traps near the edges of a pixel may affect only extremely large charge packages.

It is never possible to know exactly where the traps are within each pixel. Furthermore, this is an ever-evolving distribution. So, the AB10 model treats all pixels as having the same number and distribution of “microtraps”. To do this, they model the total number of traps (in the 2051 pixels of an average column) that affect electron packets of a particular size, and assign to each individual pixel the same number of traps, but with each trap grabbing only  $0.0004875$  ( $1/2051$ ) of an electron. The model thus has a simple list of how many traps there are per column that can affect the 1<sup>st</sup> electron in a pixel, the 2<sup>nd</sup> electron in a pixel, the 12<sup>th</sup> electron in a pixel, the 100<sup>th</sup> electron in a pixel, the 10,000<sup>th</sup> electron in a pixel, etc. All of the pixels are considered to be identical.

The other aspect of the AB10 model has to do with what happens when an electron fills a trap. There is a probability after each parallel transfer that an electron in a trap will be released into a pixel that is upstream from the pixel where it originated. The CTE model thus has two parameters:  $q(N)$ , the marginal electron that the  $N^{\text{th}}$  trap will grab, and  $\phi(j)$ , the probability that a trap will release its grabbed charge in the  $j^{\text{th}}$  shift after it was captured. The probability function  $\phi(j)$  can also be a function of packet size  $q$ ,  $\phi(j;q)$ , but the initial WFC3/UVIS study suggested that there was no dependence on  $q$ .

The current CTE model was constructed based on data taken in December of 2016. The model was largely based on the approach in AB10, wherein the trails behind warm pixels (WPs) in the darks were examined in order to infer the amount of charge lost from the WP itself. This is an indirect way of measuring the losses. It is particularly hard to do this for small packets, since the wispy trails are very easy to lose in the noise.

The new model makes use of a more direct approach, at least for the parameters of the model that deal with small packets. We first take some long 900s darks with a good level of post-flash, and correct these images with the best available pixel-based CTE reconstruction model. This allows us to identify all the WPs and measure an intensity for each. We also take a series of short  $\sim 30$ s darks with various levels of post-flash. We scale down the flux in each WP from the long darks by a factor of 30 to determine how many electrons each WP *should* have started out with in the short darks. We then examine WPs at the top of the detector that have had to undergo  $\sim 2000$  parallel shifts, and thus lose a lot of their electrons. We study how the loss observed for each WP varies depending on the background level. Generally, when the background rises, a WP sees fewer

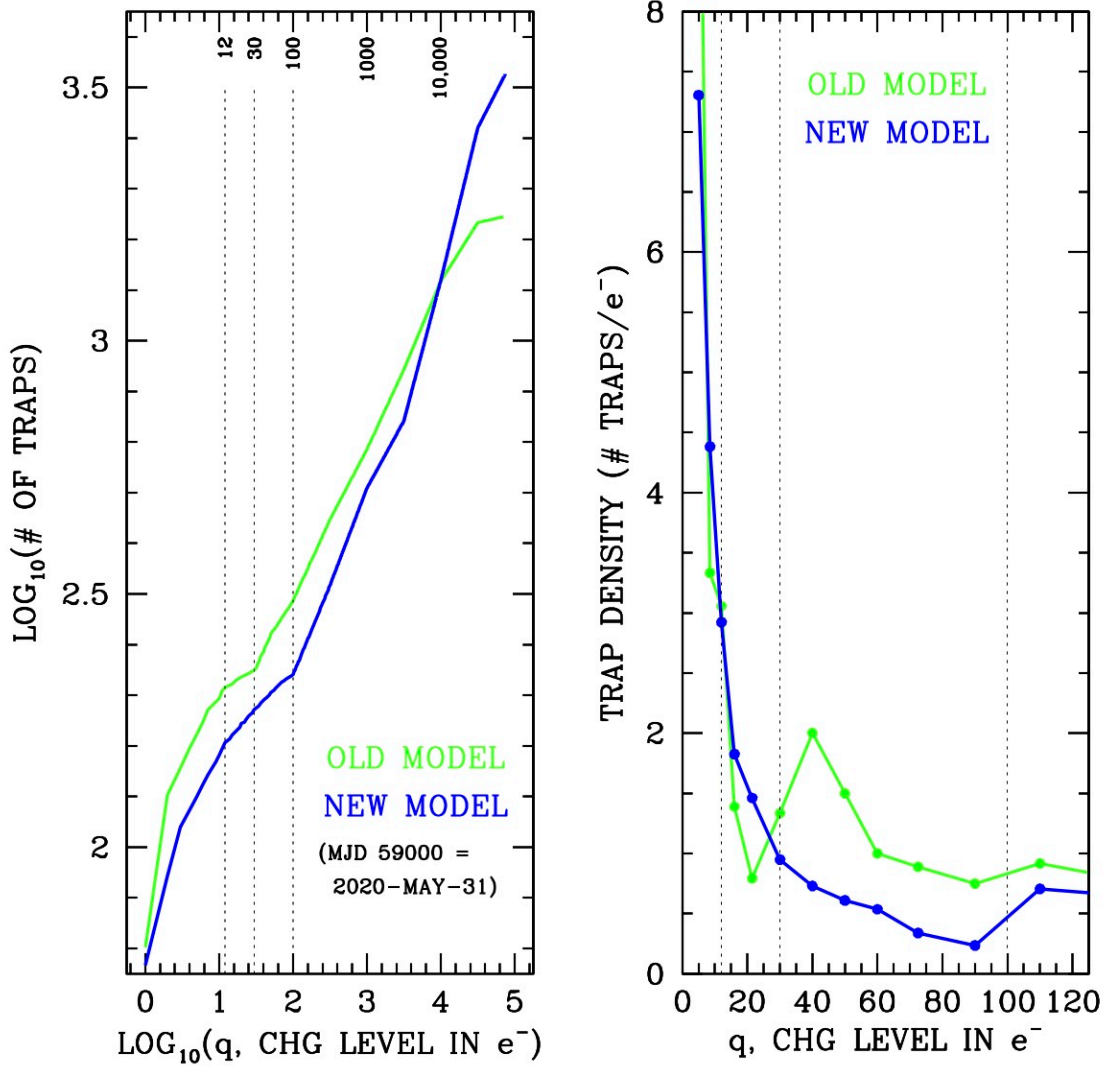


**Figure 1:** On the left, we plot trap number  $N$  as a function of  $q$ , the marginal electron that the trap interacts with, for the old and new models. The number of traps corresponds to the total in a 2051-pixel column. On the right, we show a differentiation of the model, showing the number of traps that can affect each marginal electron in a pixel packet. Both models are projected forward in time to correspond to 31 May 2020, MJD 59000.

traps and preserves more of its charge. By examining this relationship in detail, we can directly measure the “trapping” part of the model,  $q(N)$ . (The previous model actually had did have access to the some long-short data to pin  $q(N)$  below packet sizes of  $15 e^-$ , but above this we had to rely on the “indirect” method of measuring the losses by measuring the trail.

The data for the new model involved studying how backgrounds from  $0 e^-$  to  $50 e^-$  affect the CTE losses of small warm pixels. Since we were able to examine  $q(N)$  directly, without reference to the trails, we could then independently measure the release part of the model,  $\phi(j)$ , from the trails. This has allowed us to see for the first time that the trail-release profile  $\phi(j)$  is actually much steeper for small packets ( $q < 90 e^-$ ). Both of these insights together imply a different curve for  $q(N)$  for small electron packets. **Figure 1** compares the old model with the new one.

The limited data we had in-hand for the 2016 model seemed to imply that there was a “sweet spot” between packet sizes of 12 electrons and 30 electrons. Now that we have more WPs to study, a stronger CTE signal, and better optimized calibration data, we are able to verify that the losses below a background of 12 electrons are indeed grave. But there is actually no magic plateau. The losses simply go down steadily as the packet size grows from 12  $e^-$  to 100  $e^-$ . The old model (in green) predicts more traps and thus much larger losses for these packets. This can be traced to the “indirect” way we had to infer  $q(N)$  from the trails under the faulty assumption that all trails have the same shape. It was very hard to “see” the extended trails for faint WPs.

Above 100 electrons, the two models are very similar, except at the very brightest end (above  $10^4$  electrons). We now have twice as many super bright WPs and thus we can do a better job characterizing CTE losses for the largest pixel packets.

The upcoming ISR (Anderson 2020) will do a more thorough job describing the derivation of the new model. In the next few sections, we will show some empirical demonstrations of the “state of the CTE” in order to help GOs understand how to plan their observations wisely.

### 3. Implications of the new model

The main difference between the old and new model is that we now know that there is no “sweet spot” at a background of 12  $e^-$ . It is still true that below this background, CTE losses increase precipitously. But now we know that if users increase the background beyond 12  $e^-$ , they will mitigate CTE losses even more. One could see this as a downside, but this is really an opportunity that allows users an extra dimension of phase space to explore in planning their observations.

The model itself does not directly tell users what background to use. It is convenient to examine the data directly to visualize the survival of WPs as a function of background level. We will start with calibration data based on WPs, then we will examine what imperfect CTE does to actual stars.

Cal Program 16029 (PI-Anderson) was performed to provide data on the efficacy of various post-flash levels in suppressing CTE losses. We took a series of thirty 20-second darks with POSTFLASH levels between 0 and 36 electrons, and sixteen identical 900-second darks with a POSTFLASH of 12  $e^-$ .

We stacked the CTE-corrected 900-s darks, identified WPs, and determined an intensity for each. We then scaled each WP down by a factor of 45 to construct an estimate of how many counts the WPs in the 20-second darks<sup>1</sup> should have started with. A WP with 135  $e^-$  in the long exposures will have only  $\sim 4$  counts in the short darks. By examining these ultra-low WPs, we can get a handle on the marginal charge loss<sup>2</sup> at each background level. It is the marginal charge loss that tells us how the faintest measurable sources are impacted by CTE.

---

<sup>1</sup> Note that to ensure that all the post-flashed darks have the same effective dark time, we had to consider how long the post-flashing and commanding would take and subtract that off from the commanded dark time.

<sup>2</sup> Note that by studying WPs with intensities of 25 or so, the WP is not probing the number of traps at a single background level, but rather the number of traps that impact a range of packet sizes.

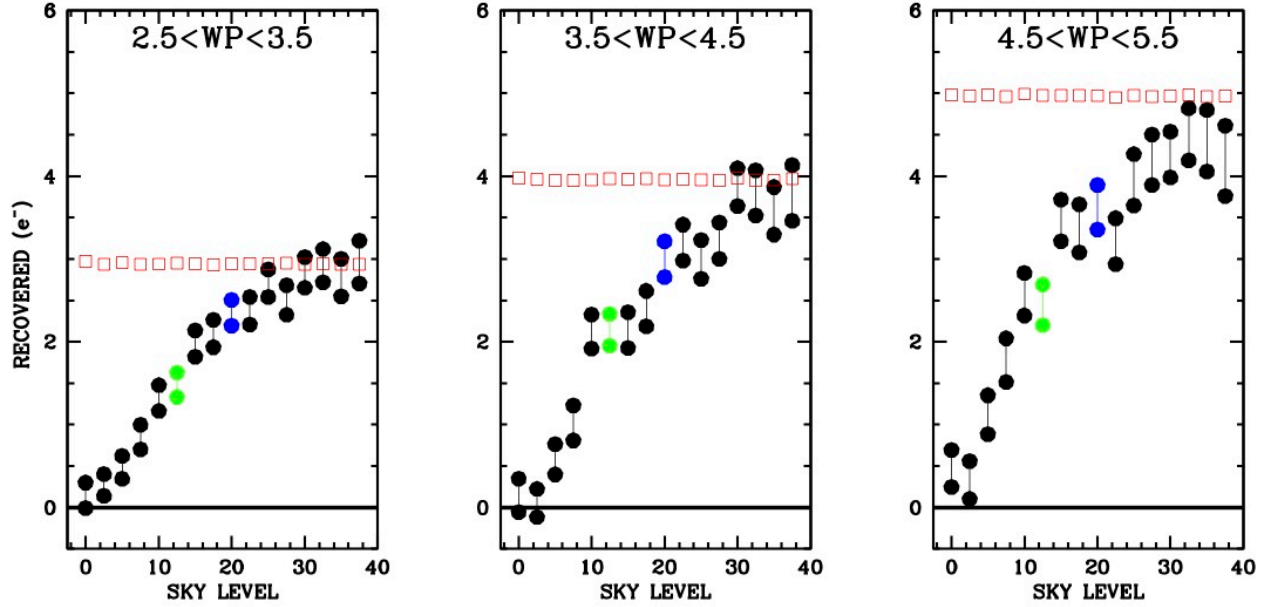


**Figure 2:** The number of electrons received at the readout register from 3, 4, and 5  $e^-$  WPs after 1500 to 2000 parallel transfers to the readout register. The red squares are indicative of the original number of electrons in each WP.

**Figure 2** shows the survival intensities of WPs transferred from the top quarter of the detector ( $1500 > j > 2000$ ) at a variety of background levels. We divided the WPs into three bins, centered on initial WP intensities of 3, 4, and 5 electrons. It is clear that when the background is very low, almost no electrons from any of the WPs survive. When the background is 12  $e^-$  (the green points) about 50% of the charge survives. When the background is about 20  $e^-$  (the blue points) about 75% of the charge survives. As the background increases to 30  $e^-$  the surviving flux continues to increase. The three panels show similar results.

These plots should be considered more qualitative than quantitative, since there is some uncertainty in the exact starting number of electrons in each WP, since we are extrapolating from a stack of long dark observations that had themselves to be corrected for CTE. But the trends are very clear: we definitely get better transfer with higher background levels. There is no “sweet spot” at 12  $e^-$ , but rather it is the start of a more gradual improvement in transfer efficiency.

**Figure 3** provides a summary of the three panels in **Figure 2**. It is indeed curious that it appears that we get over to 90% transfer for sky levels above 30  $e^-$ . The model in **Figure 1** certainly does not predict such high transfer at this level. The model does show that marginal losses at a background of 20  $e^-$  should be 50% less than those at 12  $e^-$ , which is what we see here. But according to **Figure 1**, a background at 30  $e^-$  should be only about 30% better than that a background at 20  $e^-$ ; here we see considerably more improvement.

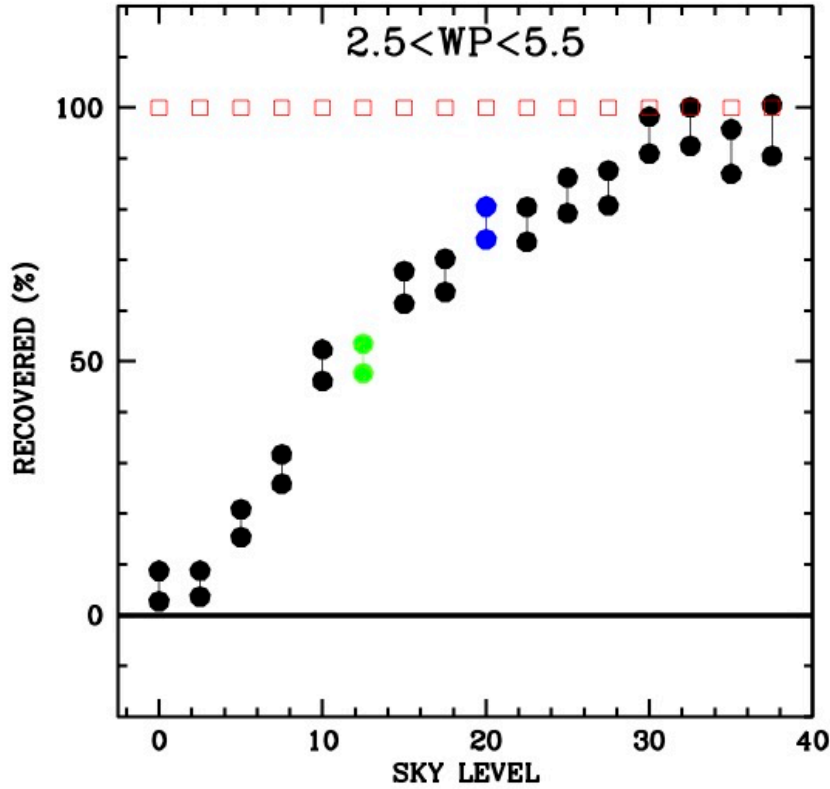
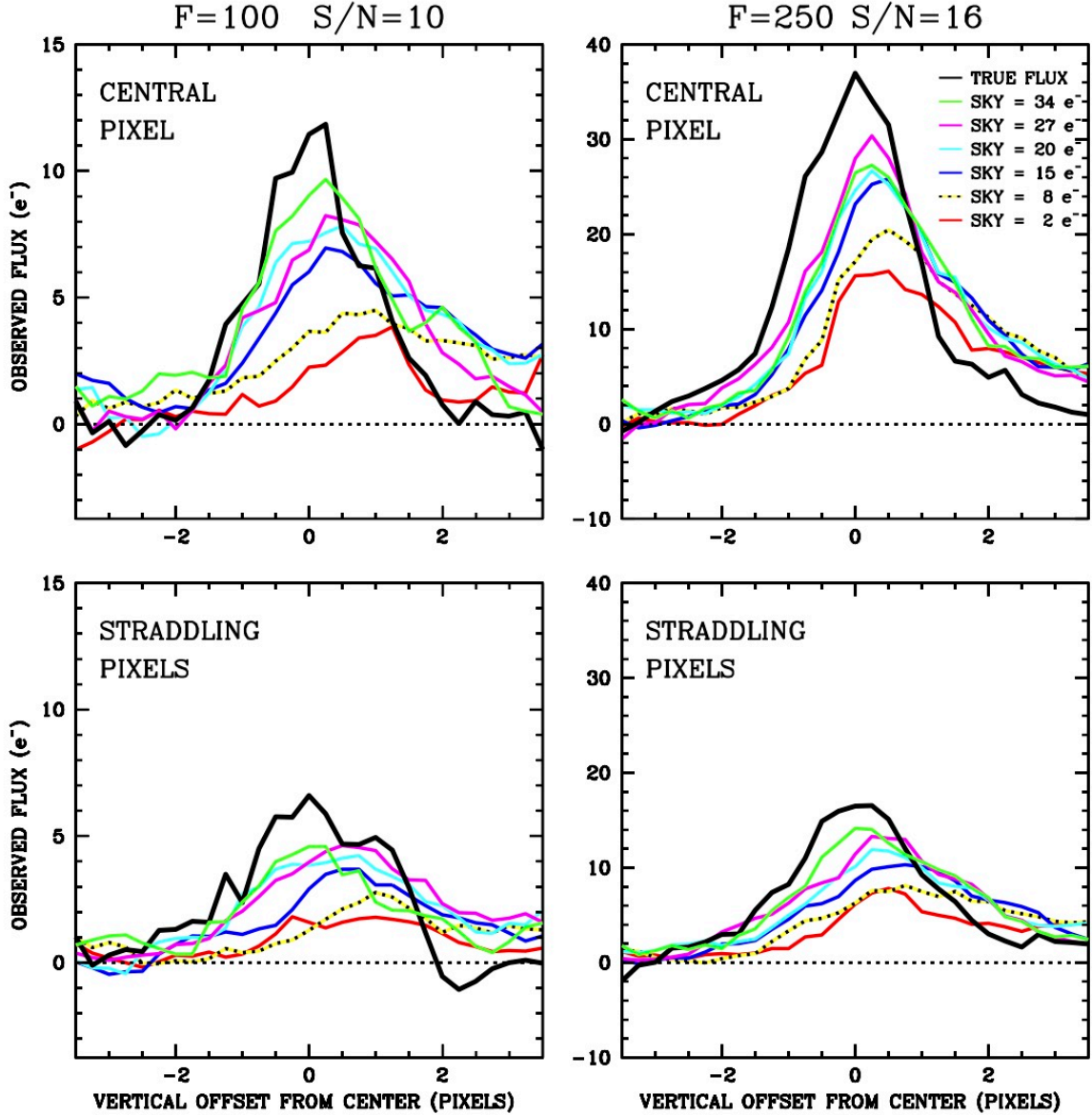


Figure 3: The average fraction of recovered electrons for “marginal” electrons parallel transferred from near the top of the detector to the readout register as a function of sky background. See text for an explanation as to why the 90% transfer above backgrounds of 30 may apply only to marginal electrons but definitely not apply to all added electrons.

One possible explanation is that Poisson noise should make the sky background non-uniform, such that that a background of  $25\text{ e}^-$  really has pixels of  $25 \pm 5$  electrons in a WP’s downstream pixels. There’s a good chance that even after the 3 to  $5\text{ e}^-$  get added at the location of the WP, there are still some higher pixels nearby that may end up filling some of the traps that the WP would otherwise see if the background had been perfectly flat. Now, if the WP had 25 extra electrons on top of a “forest” of  $25\text{ e}^-$ , then the WP would stand up above all the other trees and get cut down much more rapidly. At the moment, this is all conjecture, but we plan to test this. It could have some encouraging implications for WFC3/UVIS’s ability to detect marginal sources.

It is worth repeating that the high transfer efficiency seen for backgrounds between  $30\text{ e}^-$  and  $40\text{ e}^-$  do *not* imply vanishingly small CTE losses for brighter sources at these moderately high backgrounds. There are some traps in the lattice that affect only electron clouds that have more than  $50\text{ e}^-$ , and some that will affect only clouds with more than  $100\text{ e}^-$ , and some that affect only clouds larger than  $10,000\text{ e}^-$ . Higher backgrounds cannot protect against these losses. Higher backgrounds can offer significant protection only for faint sources.



**Figure 4:** The vertical profiles of faint stars (left) and medium-bright stars (right) in the upper quarter of the detector ( $1500 > j > 2000$ ) on a variety of background levels. The charge-shuffle direction is leftward in these plots.

Of course stars are different from WPs. The WFC3/UVIS detector is undersampled, but only moderately so. A star's central pixel collects  $\sim 16\%$  of the total flux and the adjacent pixels  $\sim 9\%$ . The downstream pixels of a star thus provide a significant natural buffer against CTE losses.

**Figure 4** provides a direct window into how various background levels protect stars against significant CTE losses. These four plots represent a composite comparison of many stars observed in short exposures with various levels of background, using their known brightnesses and positions from deeper exposures. The two panels on the left show a relatively faint star with  $\sim 100$  electrons total ( $S/N \sim 10$ ). The black curves show that such a star should have about 16 electrons over sky in its central pixel. The right panels show a brighter star with  $\sim 250$  electrons



total ( $S/N \sim 16$ ). The top panels show the vertical profile through the stars' central column of pixels, and the bottom panels show the pixels in the columns  $\pm 1$  pixel to the right or left.

The ravages of imperfect CTE are obvious. The electrons of the star start getting grabbed by the traps at the downstream end (to the left on the x-axis of the plots) and sometimes get released on the right-hand side of the profile. Sometimes the grabbed electrons get released well outside of the window shown.

It is easy to see how an extremely low background ( $2 e^-$ , red curve) almost *completely* erases the presence of a faint star from where it is supposed to be. Only about 25% of the original electrons end up within a 2-pixel-radius aperture. It is worth noting that these losses are considerably more modest than what we saw above with marginal WPs, where only about 5% of the WP flux made it out with the pixel. Here, we retain  $5\times$  more flux. This is some of the natural protection that a star's outer pixels provide for it.

Increasing the sky value allows more and more of the star's flux to be preserved and remain with the pixel where it originated. Note that the star's centroid is noticeably displaced vertically by this process but not so much so that it would be carried out of a reasonable aperture. The shape of the star is broadened in the vertical direction as well.

It is clear from these plots that there is no "optimal" level of background to add. Increasing the background from  $8 e^-$  to  $15 e^-$  results in improved transfer, as does increasing it from  $15 e^-$  to  $20 e^-$ ,  $20 e^-$  to  $27 e^-$ , and  $27 e^-$  to  $34 e^-$ . This is the case both for the star's central column as well as for the pixels in columns to the right and left (the two of which together contain just as much signal as the star's central column of flux).

It is worth noting that when the brightness of the star increases from  $100 e^-$  to  $250 e^-$  total (an increase of one magnitude), much more of the star's flux is preserved, even in the low sky case. Once the background reaches about  $15 e^-$ , we don't see much of a difference in how much the background protects losses in the central column (top-right plot). In the flanking columns (bottom-right plot), the background makes even more of a difference. This is consistent with what we observed earlier: increasing the background mostly helps the lower-valued pixels.

We did not have enough sources fainter than  $100 e^-$  total flux to explore an even fainter magnitude bin. Recall that [Figure 3](#) hinted that sources that were close to the level of the Poisson noise in the background may experience lower losses. We have calibration data coming soon that should help us answer this question.



## 4. Recommendations for planning future observations

The best thing observers can do to deal with potential CTE issues is to minimize losses in the first place. The main strategies for this were discussed in the initial White Paper<sup>3</sup> on the subject by MacKenty and Smith. Section 6.9.2 of the WFC3 instrument handbook also provides many options for CTE-loss avoidance. We summarize the basics here, but users should avail themselves of other resources as well.

One strategy is to divide the observations in to fewer — but longer — exposures. This has several benefits. First, it provides more natural background, so that less post-flash will be required to achieve the desired CTE-mitigation level. Second, it increases the source signal per exposure relative to the readnoise *and* relative to whatever post-flash is used. Finally, each readout avoided adds 90+ seconds to the total exposure time available. The downside, of course, is that fewer dithers provide less mitigation from image defects and CRs and also allow fewer sub-pixel samplings of the scene, which can limit the achievable resolution through `Drizzle` reconstruction. That said, users who plan several orbits of identical observations of the same scene in order to go super deep often use only two or even just one exposure per orbit<sup>4</sup> in order to lessen the impact of CTE losses.

Another strategy to lessen CTE losses is to place the target closer to the readout amplifier. This of course cannot be done if the target takes up the full 164"×164" field of view, but it is possible for smaller targets. This can be done with either the subarrays (UVIS2-C512C-SUB and UVIS2-C1K1C-SUB) or by placing the target closer to the readout, even while reading out the entire detector (i.e., with the “CTE” apertures).

Post-flash is, of course, a final option. APT allows post-flash levels from 0 to 25 electrons to be set by observers. The WFC3 ETC (<https://www.stsci.edu/hst/instrumentation/wfc3/software-tools/exposure-time-calculators>) or ISR-2012-12<sup>5</sup> by Baggett and Anderson provides estimates of the natural background level per second for typical blank fields for most of the UVIS filters. Of course, the image background can be larger than this if there is an extended object present. Users should obtain the best estimate of the expected background so that they post-flash only as much as is truly needed to mitigate CTE.

---

<sup>3</sup>See: [https://www.stsci.edu/files/live/sites/www/files/home/hst/instrumentation/wfc3/performance/cte/\\_documents/CTE\\_White\\_Paper.pdf](https://www.stsci.edu/files/live/sites/www/files/home/hst/instrumentation/wfc3/performance/cte/_documents/CTE_White_Paper.pdf)

<sup>4</sup>Whole-orbit exposures have a lot of CRs and a minimum of 8 exposures are needed to allow for effective mitigation (Marc Rafelski, personal communication). There is also a bit more blurring of the PSF than typical in the longer exposures. See also program GO-13872 by Oesch for another example.

<sup>5</sup>See: [https://www.stsci.edu/files/live/sites/www/files/home/hst/instrumentation/wfc3/documentation/instrument-science-reports-isrs/\\_documents/2012/WFC3-2012-12.pdf](https://www.stsci.edu/files/live/sites/www/files/home/hst/instrumentation/wfc3/documentation/instrument-science-reports-isrs/_documents/2012/WFC3-2012-12.pdf)

The information in Sections 2 and 3 was provided to help users understand what imperfect CTE does to observations. Previously, we were able to issue guidance that post-flashing to ensure a relatively harmless background of  $12\text{ e}^-$  should provide adequate protection against losses. At the time, the losses at this background level were less than 25%, and this was a perturbation that the pixel-based model could safely reconstruct. With the continuing damage to the detector, marginal losses at this background level have now increased to about 50%. This is too large to correct in an automated way, and moreover, it results in significant S/N loss. Even a perfect reconstruction algorithm cannot restore lost S/N.

The good news is that it is possible to increase the background level beyond  $12\text{ e}^-$  to gain considerable additional protection. The “bad” news is that there is no one-size-fits-all recommendation. Users will have to combine the information above with the details of their scene, their target, and their observational goals to determine which background level works best for them. The choice of how much post-flash background to add is a cost-benefit analysis to optimize the signal to noise. Increasing the background increases the signal, but it increases the noise, as well. It is worth remembering that it is the faintest sources of interest that are most sensitive to this calculation.

The plots in [Figure 4](#) should provide the most direct possible estimate of what CTE inefficiencies do to faint objects with  $S/N \sim 10$  per exposure. A background increase from about  $12\text{ e}^-$  to  $20\text{ e}^-$  could cut the CTE losses for such a star by 50%. [Figure 3](#) shows that objects with  $S/N \sim 1$  per exposure that can be detected only by combining multiple exposures should also benefit from more post-flash in the  $20\text{ e}^-$  range, but of course a careful balance of preserved signal and added noise will still be required.

Finally, it is worth underlining that increasing the background will *not* have a large effect on the CTE losses for bright stars. These stars will continue to experience some CTE losses even with backgrounds upwards of  $100\text{ e}^-$ . [Figure 1](#) shows that a pixel with  $400\text{ e}^-$  will have to deal with twice as many traps as a pixel with  $100\text{ e}^-$ . If we add the  $400\text{ e}^-$  pixel to a background of  $100\text{ e}^-$ , then that will only spare it from about half the traps, while at the same time adding additional noise from the flash.

## 5. References

Anderson, J & Bedin, L. R. 2010 PASP 122 1035-1064: *An Empirical Pixel-Based Correction for Imperfect CTE. I. HST’s Advanced Camera for Surveys*